WPEDU-PR(18) 21274

MS Anastopoulos Tzanis et al.

Non-Axisymmetric Equilibrium and Stability using the ELITE Stability Code

Preprint of Paper to be submitted for publication in
Nuclear Fusion

This work has been carried out within the framework of the EUROfusion Consortium and has received funding from the Euratom research and training programme 2014-2018 under grant agreement No 633053. The views and opinions expressed herein do not necessarily reflect those of the European Commission.

This document is intended for publication in the open literature. It is made available on the clear understanding that it may not be further circulated and extracts or references may not be published prior to publication of the original when applicable, or without the consent of the Publications Officer, EUROfusion Programme Management Unit, Culham Science Centre, Abingdon, Oxon, OX14 3DB, UK or e-mail Publications.Officer@euro-fusion.org

Enquiries about Copyright and reproduction should be addressed to the Publications Officer, EUROfusion Programme Management Unit, Culham Science Centre, Abingdon, Oxon, OX14 3DB, UK or e-mail Publications.Officer@euro-fusion.org

The contents of this preprint and all other EUROfusion Preprints, Reports and Conference Papers are available to view online free at http://www.euro-fusionscipub.org. This site has full search facilities and e-mail alert options. In the JET specific papers the diagrams contained within the PDFs on this site are hyperlinked

Non-Axisymmetric Equilibrium and Stability using the ELITE Stability Code

M.S. Anastopoulos-Tzanis [1,2], B.D. Dudson [1], C.J. Ham [2], C.C. Hegna [3], P.B. Snyder [4], H.R. Wilson [1,2]

1) York Plasma Institute, Department of Physics, University of York, York, YO10 5DD, UK
2) Culham Centre for Fusion Energy, Abingdon, Oxon OX14 3DB, UK
3) Departments of Engineering Physics and Physics, University of Wisconsin-Madison, Madison, Wisconsin 53706, USA
4) General Atomics, San Diego, California 92186-5608, USA

October 2018

Abstract. A linear perturbation theory is used to model the MHD stability of tokamak equilibria under the application of external 3D magnetic perturbations [C.C. Hegna, *Physics of Plasmas* **21**:072502, 2014]. The symmetry breaking produces the coupling of toroidal n modes. We use ELITE [H.R. Wilson et al., *Physics of Plasmas* **9**:1277, 2002] to produce both a linearly perturbed non-axisymmetric equilibrium state as well as the linear axisymmetric modes, that are coupled for the stability analysis. The symmetry breaking produces coupling of modes with different toroidal mode number n and poloidal localisation of the non-axisymmetric peeling-ballooning mode is observed in comparison to the axisymmetric case.

1. Introduction

The efficient production of fusion power requires large pressure at the plasma core while retaining low pressure at the plasma edge, such that plasma facing components (PFCs) operate in an acceptable environment. Such pressure profiles are observed in high confinement mode (H-mode) plasmas. However, the establishment of a steep pressure gradient at the edge, so called pedestal region, together with large bootstrap driven edge current density is potentially destabilising for peeling-ballooning (PB) instabilities [1]. Those instabilities are manifested as edge localised modes (ELMs) and correspond to rapid bursts of particles and heat to PFCs, especially to the divertor of the reactor. For large tokamaks like ITER, those transients will result in heat fluxes that exceed the melting point of tungsten [2], the main material of the divertor tiles. Therefore, active ELM control methods are required to minimise potential damage of the reactor [3].

One method of ELM control that is widely applied to devices around the world and will be installed in ITER, uses external non-axisymmetric resonant magnetic perturbations (RMPs) produced from magnetic coils placed inside the tokamak vessel.

Experimental observations indicate two main operational states, one with ELM mitigation and the other with complete ELM suppression. In mitigation, a decreased energy loss per ELM ΔW_{ELM} leads to an increase of ELM frequency f_{ELM}. For ITER-like shape low density $n/n_{GW} \sim 0.3$, where $n_{GW} = I_p/\pi a^2$ is the Greenwald density limit, and low collisionality $\nu^* = \nu_{ei}\sqrt{m_e/k_B T_e}\epsilon^{-3/2}qR \sim 0.01$, complete suppression has only been observed at DIII-D [4] and recently in AUG [5], while for higher collisionality $\nu^* \sim 1$ KSTAR [6] has also achieved ELM suppression. The exact physics mechanism that allows this ELM free regime is still to be understood. In addition, ITER will operate in a high density $n/n_{GW} \sim 0.7$ low collisionality $\nu^* \sim 0.01$ regime such that extrapolation from current machines could be challenging in the absence of a rigorous physics basis.

In general, external 3D fields affect transport and MHD properties of the plasma. The resonant component of the field drives current structures at rational surfaces that can in turn lead to magnetic islands that greatly increase perpendicular transport [7],[8],[9]. As a result, the pressure gradient in the pedestal is relaxed and global stability boundaries are not exceeded. However, plasma flow that exists in the pedestal region can be strong enough that island structures could heal [10],[11]. In addition, the geometrical change of the equilibrium can affect MHD instabilities leading to potential modification of stability boundaries that can directly affect the onset of ELMs. Ideal infinite-n ballooning analysis reveals that the dominant effect of the applied 3D is to alter the local shear, which has significant consequences for local MHD stability [12],[13],[14]. However, for intermediate-n modes responsible for the occurrence of ELMs, a global 3D analysis is needed. However, global 3D stability codes that already exist [15],[16] have not yet been applied to an RMP ELM control scenario. To some extent, such an investigation has been performed by non-linear fluid codes and mode coupling was observed to be one of the key mechanisms to achieve a suppressed operational regime [17].

This work focuses on the impact of toroidal symmetry breaking on the ideal MHD stability of the plasma. In a toroidally axisymmetric system the toroidal variation of the response is described by linearly decoupled discrete toroidal modes, i.e. toroidal mode number n, is a good quantum number and only poloidal coupling occurs. Considering an additional non-axisymmetric part of the equilibrium that is much smaller than the axisymmetric part, typically $\delta B/B \sim 10^{-4}$, together with approximately retained nested flux surfaces, linear perturbation theory can be employed to provide the required geometrical coupling of the axisymmetric modes. This coupling will result in energy transfer between neighbouring toroidal Fourier modes that can directly affect the evolution of instabilities. In this paper, we will explore this coupling mechanism.

2. Perturbative Ideal MHD Stability

A perturbative stability analysis was performed to first order in Ref.[18] and then to second order in Ref.[19]; this is required to capture perturbative non-axisymmetric

effects. Considering the force-balance equation,

$$-\omega_n^2\vec{\xi}_n = (\mathbf{F} + \delta\mathbf{F})\vec{\xi}_n \tag{1}$$

where ω_n^2 is the real eigenvalue of the system, the force operator can be separated into an axisymmetric part $\mathbf{F}$ and non-axisymmetric part $\delta\mathbf{F}$ part; provided $\mathbf{F} \gg \delta\mathbf{F}$, the non-axisymmetric force can be treated as a perturbation. The axisymmetric operator $\mathbf{F}$ is Hermitian and provides the equation for the unperturbed system which corresponds to the 0^{th} order equation,

$$-\omega_{n0}^2\vec{\xi}_{n0} = \mathbf{F}\vec{\xi}_{n0} \tag{2}$$

and a spectrum of real eigenvalues ω_{n0}^2 arises, provided that $(\vec{\xi}_{n0}, \vec{\xi}_{m0}) = \delta_{nm}$, where $(a, b) = \int a^* b dV$. The solution $\vec{\xi}_n$ of the perturbed system can be approximated by a superposition of orthogonal eigenfunctions $\{\vec{\xi}_{n0}, \vec{\xi}_{n1}, \vec{\xi}_{n2}, ...\}$ and eigenvalues $\{\omega_{n0}^2, \omega_{n1}^2, \omega_{n2}^2, ...\}$ that correspond to solutions of the relevant ordered equation projected on the unperturbed sate $\vec{\xi}_{n0}$. The 1^{st} order equation,

$$-\omega_{n0}^2\vec{\xi}_{n1} - \omega_{n1}^2\vec{\xi}_{n0} = \mathbf{F}\vec{\xi}_{n1} + \delta\mathbf{F}\vec{\xi}_{n0} \tag{3}$$

gives a correction $-\omega_{n1}^2 = (\vec{\xi}_{n0}, \delta\mathbf{F}\vec{\xi}_{n0}) = \delta V_{nn}$ due to axisymmetric changes of the plasma equilibrium. The 2^{nd} order equation,

$$-\omega_{n0}^2\vec{\xi}_{n2} - \omega_{n1}^2\vec{\xi}_{n1} - \omega_{n2}^2\vec{\xi}_{n0} = \mathbf{F}\vec{\xi}_{n2} + \delta\mathbf{F}\vec{\xi}_{n1} \tag{4}$$

is required for the case of non-axisymmetric RMP fields and results in a correction $-\omega_{n2}^2 = (\vec{\xi}_{n0}, \delta\mathbf{F}\vec{\xi}_{n1})$. The structure of the perturbation $\vec{\xi}_{n1}$ is required and can be obtained considering Eqn.3. The orthogonal nature of a perturbation $(\vec{\xi}_{n0}, \vec{\xi}_{n1}) = 0$ implies that it can be expressed as a series, summing over a basis of the unperturbed functions $\vec{\xi}_{n1} = \sum_{m\neq n} c_{nm}\vec{\xi}_{m0}$. Projecting Eqn.3 with respect to $\vec{\xi}_{m0}$ results in an expression for $c_{nm} = -\delta V_{mn}/(\omega_{n0}^2 - \omega_{m0}^2)$, where $\delta V_{mn} = (\vec{\xi}_{m0}, \delta\mathbf{F}\vec{\xi}_{n0})$, such that the 1^{st} order correction in the displacement of a given mode is given by,

$$\vec{\xi}_{n1} = -\sum_{m\neq n} \frac{\delta V_{mn}}{\omega_{n0}^2 - \omega_{m0}^2}\vec{\xi}_{m0} \tag{5}$$

Substituting Eqn.5 into Eqn.4 and taking the inner product with $\vec{\xi}_{n0}$, provides a quantitative expression for the 2^{nd} order correction of the eigenvalue ω_{n2}^2,

$$\omega_{n2}^2 = \sum_{m\neq n} \frac{\|\delta V_{nm}\|^2}{\omega_{n0}^2 - \omega_{m0}^2} \tag{6}$$

It is interesting to note that for $\omega_{n0}^2 - \omega_{m0}^2 < 0$ the contribution is stabilising, while for $\omega_{n0}^2 - \omega_{m0}^2 > 0$ the contribution is destabilising. Therefore, for a spectrum $\omega_{n0}^2 > \omega_{m0}^2$ for $n > m$, coupling to higher modes has a stabilising contribution, while coupling to lower modes has a destabilising influence. Moreover, if the spectrum has a peak then this peak will always get more unstable.

Low-n ELITE [20],[21] is an axisymmetric MHD stability code that can very efficiently simulate the linear ideal plasma response from low to high n toroidal modes. ELITE solves the equation of motion for the normal plasma displacement functional

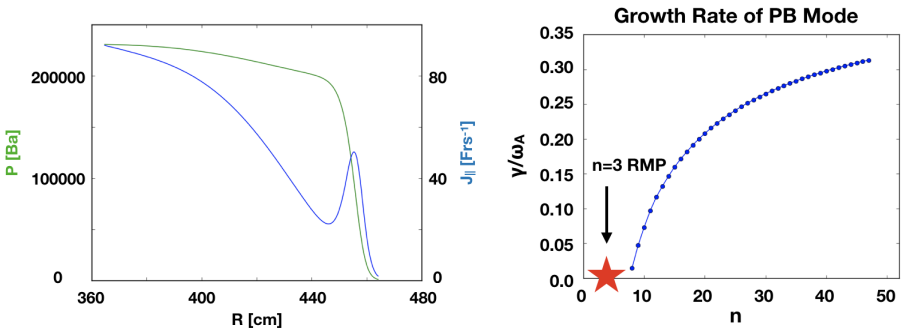

(a) (b)

Figure 1: Radial equilibrium plasma profiles for a) the pressure and current density as well as b) the normalised PB growth rate illustrating a stable equilibrium for low-n perturbations.

that minimises the axisymmetric energy principle for an ideal incompressible plasma. In such a way, PB instabilities are captured and the ideal nature of the plasma retains nested flux surfaces, which is required for the perturbative stability analysis we adopt. Consequently, ELITE can be used to provide the radial axisymmetric basis eigenfunctions and (neglecting inertia) the 3D part of the plasma equilibrium, assuming the RMP mode is stable. We aim to use ELITE for both the equilibrium (plasma response) calculation and for the stability calculation since the code is optimised for the intermediate-to-high toroidal mode numbers that interest us. This is the first stage of a project to develop a tool which can optimise plasma response and ELM stability together.

3. Application to RMPs

The calculation of the non-axisymmetric part of the equilibrium requires an initial axisymmetric equilibrium that is stable to low-n toroidal modes, to be driven by RMP fields. We examine such an equilibrium here for a large aspect ratio circular cross-section plasma. The axisymmetric equilibrium plasma profiles and PB stability analysis are illustrated in Fig.1. The coordinate system used is orthogonal and based on the original axisymmetric equilibrium state (ψ_0, χ_0, ϕ), where ψ_0 is the normalised poloidal flux, χ_0 is the poloidal-like angle and ϕ is the toroidal angle. The perturbation is inserted into ELITE as a fixed boundary condition at the plasma-vacuum interface. Magnetic induction is used to link the normal field δB_ψ at the plasma boundary to the normal displacement ξ_ψ as given by,

$$\textbf{B.C.} \quad \xi_{\psi_m} = -i\frac{\mathcal{J}}{g_{\psi\psi}}\frac{q}{\nu}\frac{\delta B_{\psi_m}}{(m-nq)} \tag{7}$$

where $\mathcal{J}$ is the Jacobean, $g_{\psi\psi}$ is the covariant metric of the normal coordinate, q is the q-profile, ν is the local pitch and m, n are the poloidal and toroidal mode numbers. In

order to calculate the 3D equilibrium components the total perpendicular component is required. ELITE provides the poloidal harmonics of the normal displacement and the binormal displacement can be obtained considering energy minimisation [22].

Finally, screening currents that arise due to electron flow at rational surfaces, block the corresponding resonant harmonics of the applied magnetic perturbation and in the absence of resistivity lead to δ-like current layers. The calculation of those layers is subtle within a single fluid MHD model but can be analytically approximated from the jump of the first derivative of the normal magnetic field $\Delta_{mn} = [\![\partial_\psi(\delta B_\psi g^{\psi\psi}/B_\phi g^{\phi\phi})]\!]$ according to Ref.[23] and given by,

$$\mu_0 \vec{j}_{||} = i\frac{m\Delta_{mn}}{n^2 \oint B^2/|\nabla\psi|^2 \mathrm{dS}}\delta(\psi-\psi_r)e^{i(m\theta-n\phi)}\vec{B} \tag{8}$$

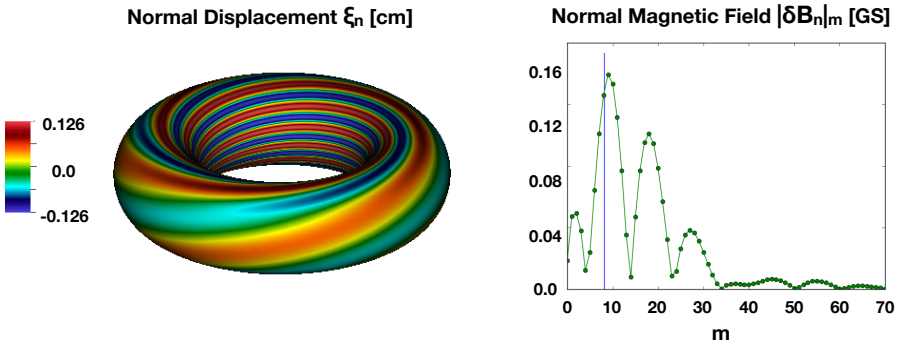

(a)

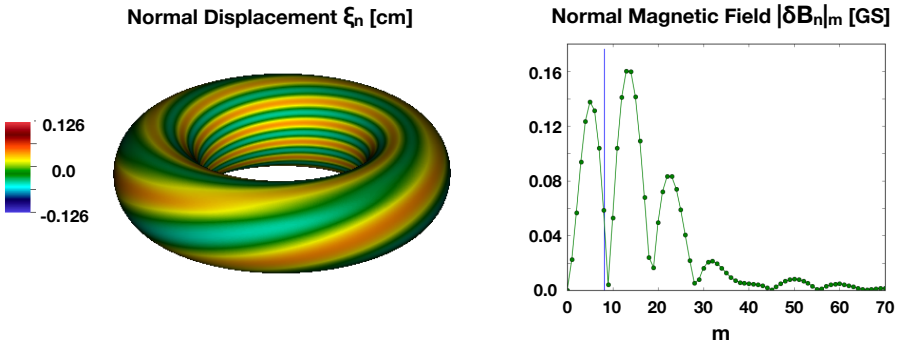

(b)

Figure 2: Normal displacement ξ_n and poloidal mode structure of normal magnetic field δB_n for the (a) resonant and (b) non-resonant N=3 RMP configuration. The solid blue line represents the resonant location $q_a N$ of the plasma surface.

3.1. Plasma Responce to RMPs

Two cases are examined for a resonant and non-resonant field at the plasma-vacuum interface for a N=3 RMP. Fig.2 illustrates the normal displacement ξ_n that represents the boundary condition and the poloidal mode structure of the corresponding normal magnetic field δB_n.

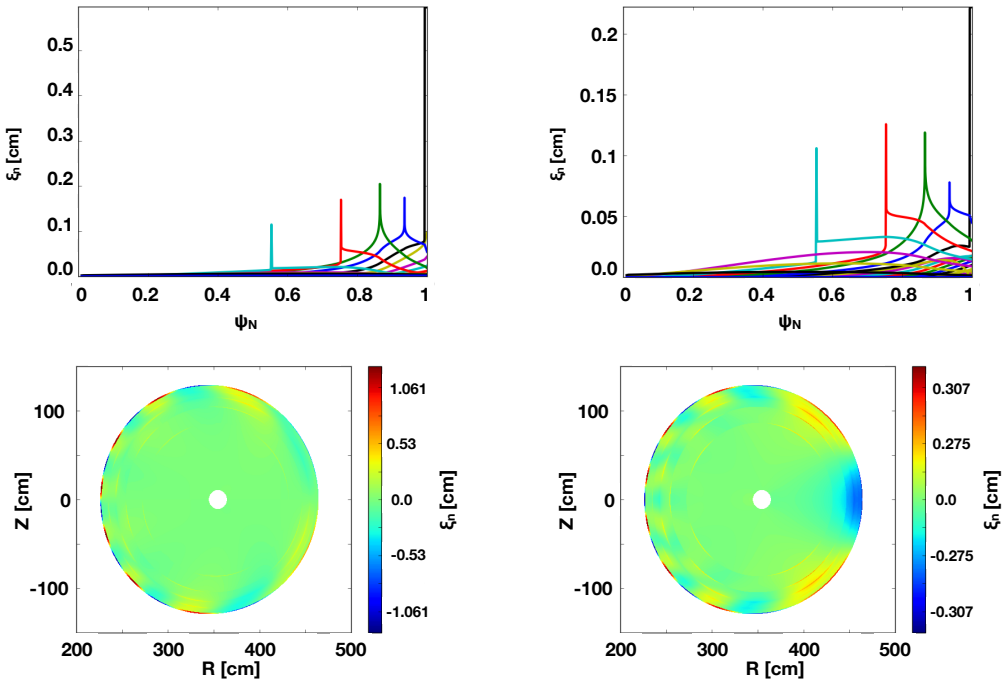

Figure 3: a) Mode structure and b) poloidal cross-section reconstruction of the normal displacement $\vec{\xi} \cdot \hat{n}$ as reconstructed from ELITE output data for an even $N = 3$ RMP case.

In the resonant case the plasma response is characterised by a strong peeling-like normal displacement, while in the non-resonant case a weaker kink-ballooning response is observed. The normal displacement is strongly peaked around rational surfaces in both cases due to resonance with the corresponding poloidal harmonics leading to large local response. Away from the rational surfaces $\vec{\xi} \cdot \hat{n} \sim \delta B_n / B$. The mode structure and the poloidal cross-section reconstruction of the normal displacement are depicted in Fig.3. The normal component of the field is imperfectly screened due to poloidal coupling in toroidal geometry, but individual modes are still screened at the corresponding rational surfaces so that island formation is prohibited in this ideal MHD model. In the non-resonant case, this screening effect is minimised since the poloidal harmonics of the magnetic field are small at the rational surfaces. However, in the resonant case the harmonics are maximised in rational surfaces and strong screening is observed leading to strong modification on the vacuum field. The normal field and its poloidal mode

structure are illustrated in Fig.4.

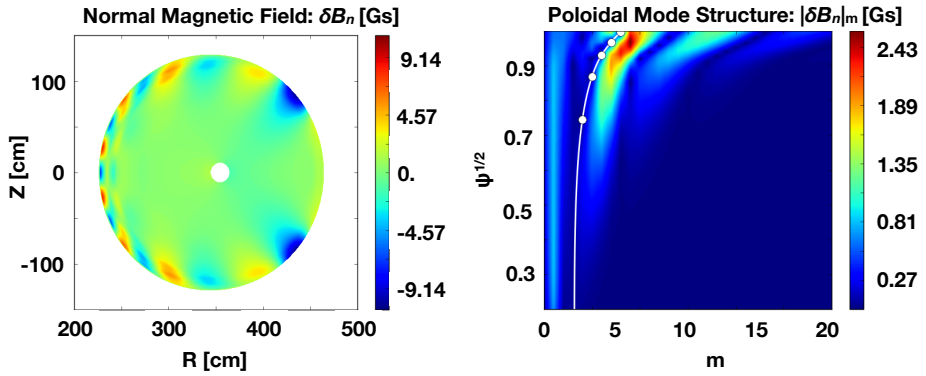

(a)

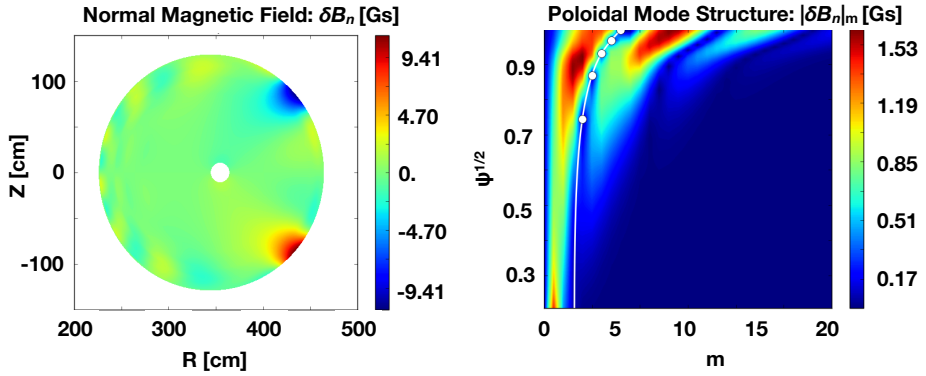

(b)

Figure 4: Normal component of magnetic field and poloidal mode structure in a straight field-line angle as reconstructed from ELITE output data for a) an resonant and b) an non-resonant n=3 RMP configuration. The straight white lines indicate the position of the magnetic coils.

Fig.5 illustrates the parallel current density created around rational surfaces, which has two contributions [24]. One contribution corresponds to the existence of Pfirsch-Schluter current density due to incompressibility and non-vanishing pressure gradient. The second contribution arises due to screening currents at rational surfaces. The ideal plasma response results in large Pfirsch-Schluter current density for both RMP configurations, which is the dominant contribution to the current density. The final perturbed equilibrium quantity needed for the coupling is the pressure gradient $\nabla\delta P$, calculated using the linearised pressure $\delta P = \vec{\xi}\cdot\nabla P_0$. The non-axisymmetric pressure profile is shown in Fig.6.

3.2. Perturbative MHD Stability

The coupling coefficients V_{nk} can be calculated using the above 3D equilibrium quantities $(\delta\vec{B}, \delta\vec{J}, \delta\vec{P})$ and axisymmetric toroidal modes $\{\vec{\xi}_{n0}\}$. Fig.7a shows the calculation

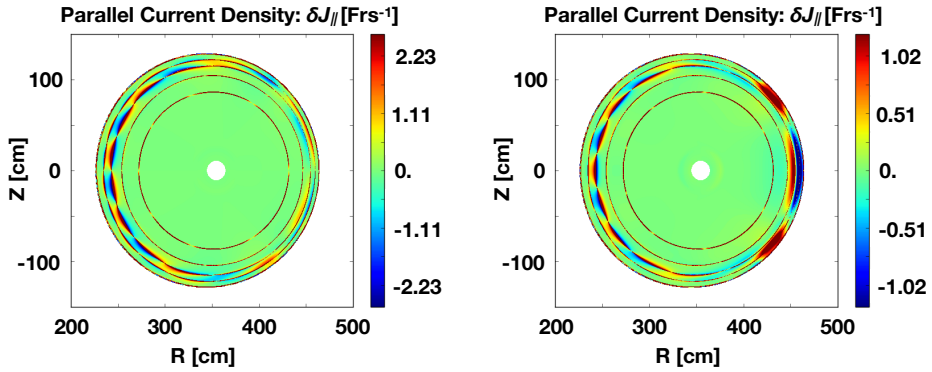

(a) (b)

Figure 5: Non-axisymmetric equilibrium parallel current density as reconstructed from ELITE for a) an resonant and b) an non-resonant n=3 RMP configuration.

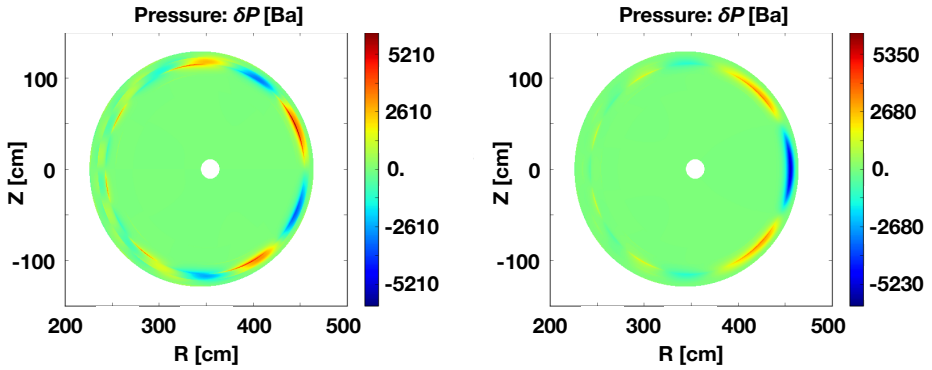

(a) (b)

Figure 6: Non-axisymmetric equilibrium plasma pressure δP as reconstructed from ELITE for a) an resonant and b) an non-resonant n=3 RMP configuration.

of the normalised growth rate of the system for the resonant and non-resonant case. Stronger coupling between the axisymmetric toroidal modes is observed at the resonant case due to larger plasma response. For this particular axisymmetric equilibrium and RMP configurations the coupling is stronger from the higher n toroidal modes such that stabilisation of the 3D growth rate is observed. Similar observations have been made qualitatively from the non-linear code JOREK [17],[25],[26]. According to those simulations, the application of RMPs lead to decreased linear growth rates and saturation of unstable modes was observed provided the applied magnetic field was strong enough to allow efficient mode coupling.

Finally, the reconstruction of the 3D normal displacement of the instability results in a localised mode structure with respect to the poloidal location, due to the interplay of different harmonics, provided that the coupling is strong enough. The 3D mode is maximised at locations where the displacement of the non-axisymmetric equilibrium

vanishes $\xi_n \sim 0$. This 3D feature has been observed experimentally and reproduced successfully be infinite-n ballooning analysis [27]. A comparison between the resonant and non-resonant case is illustrated in Fig.7b.

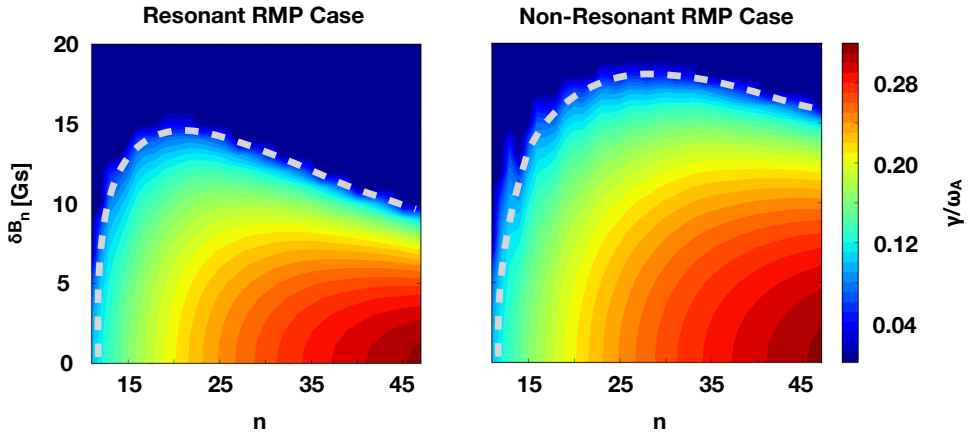

(a)

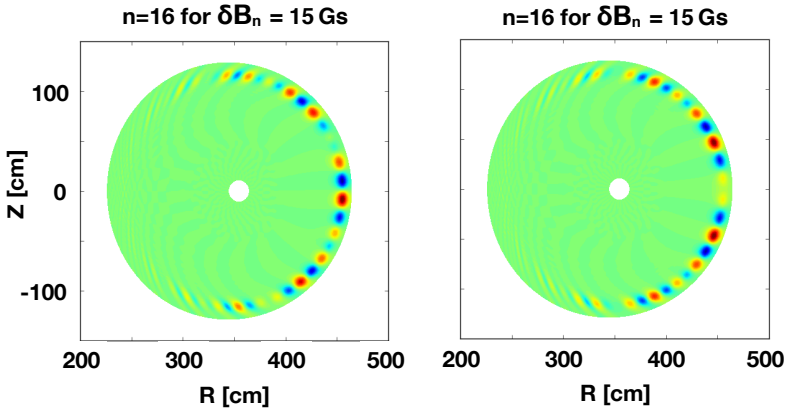

(b)

Figure 7: a) Perturbative 3D Peeling-Ballooning stability as a function of external $\delta B/B$ as reconstructed from ELITE output data. Normal plasma displacement $\vec{\xi} \cdot \hat{n}$ for a $n = 16$ 3D PB mode.

4. Conclusion

To summarise, applied RMP fields that break the axisymmetric nature of tokamak plasmas, are widely used to actively control ELMs. The 3D plasma stability can be studied in a perturbative way, as long as the full 3D equilibrium and the axisymmetric toroidal modes are known. The stability code ELITE was used to obtain both the axisymmetric toroidal eigenmodes required for the toroidal coupling and also the 3D part of the equilibrium. The 3D equilibrium was calculated by inserting a fixed boundary

condition to represent an external field. Screening current density is captured, but has not been observed to have a strong impact on MHD stability. Nevertheless, the 3D equilibrium profiles and the geometrical mode coupling had a significant impact to MHD modes above a certain phenomenological threshold for the amplitude of the applied field. Decrease of the linear growth rate was observed due to stronger coupling with the higher n sideband of the axisymmetric system, which is more unstable for ballooning modes. For cases where extrema exist in the growth rate spectrum different trends can exist. Our results share similarities with non-linear fluid simulations showing the importance of toroidal mode coupling and could provide further insight regarding the dominant physics mechanism that allows an ELM free operational state necessary for the advanced operation of ITER.

Acknowledgements

This work has been carried out within the framework of the EUROfusion Consortium and has received funding from the Euratom research and training programme 2014-2018 under grant agreement No 633053 and from the RCUK Energy Programme [grant number EP/P012450/1]. To obtain further information on the data and models underlying this paper please contact PublicationsManager@ccfe.ac.uk*. The views and opinions expressed herein do not necessarily reflect those of the European Commission. This research is supported in part by the U. S. Department of Energy (DOE) Office of Fusion Energy Sciences under grant no. DE-FG02-86ER53218.

References

[1] J.W. Connor et al., *Physics of Plasmas* **5:2687**, 1998
[2] R.A. Pitts et al., *Journal of Nuclear Materials* **438:48**, 2013
[3] A. Loarte et al., *Nuclear Fusion* **54:033007**, 2014
[4] T.E. Evans et al., *Nuclear Fusion* **48:024002**, 2008
[5] W.A. Suttrop et al., *Nuclear Fusion* **58:096031**, 2018
[6] Y. M. Jeon et al., *Physical Review Letter* **109:035004**, 2012
[7] R. Fitzpatrick, *Nuclear Fusion* **33:7**, 1993
[8] R.D. Hazeltine et al., *Physics Review Letter* **37:102**, 1976
[9] I. Joseph et al., *Nuclear Fusion* **48:045009**, 2008
[10] Y.Q. Liu et al., *Nuclear Fusion* **51:083002**, 2011
[11] M. Becoulet et al., *Nuclear Fusion* **52:054003**, 2012
[12] T.B. Cote et al., *Nuclear Fusion* **102658.R1**, 2018
[13] T.M. Bird et al., *Nuclear Fusion* **53:013004**, 2013
[14] C.J. Ham et al., *Physics of Plasmas* **21:102501**, 2014
[15] E. Strumberger et al., *Nuclear Physics* **57:016032**, 2017
[16] T. Weyens et al., *Physics of Plasmas* **21:042507** 2014
[17] F. Orain et al., *Plasma Phys. Controlled Fusion* **57:014020**, 2015
[18] P. Helander et al., *Physics of Plasmas* **20:062504**, 2013
[19] C.C. Hegna, *Physics of Plasmas* **21:072502**, 2014
[20] H.R. Wilson et al., *Physics of Plasmas* **9:1277**, 2002
[21] A.E.L. Lunniss, *University of York* **PhD Thesis**, 2016

[22] J.W. Connor et al., *Proceedings of the Royal Society London A* **35**, 1979
[23] J.K. Park et al., *Physical Review Letter* **99:195003**, 2007
[24] P. Helander, *Reports on Progress in Physics* **77:087001**, 2014
[25] F. Orain et al., *26th IAEA Fusion Energy Conference*, 2016
[26] F. Orain et al., *44th EPS Conference on Plasma Physics*, 2017
[27] M. Willensdorfer et al., *Physical Review Letter* **119:085002**, 2017